Effect of Metal-doping of Nanoscale Maghemite on Cr(VI) Adsorption and Nanoparticle Dissolution

Jing Hu, Irene M. C. Lo and Guohua Chen

Environmental Engineering Program
Hong Kong University of Science and Technology

Presented at the International Congress of Nanotechnology, October 31-November 3, 2005 San Francisco

Outline

- Introduction
- Objectives
- Methodology
- Results and Discussions
- Conclusions

Introduction

- Hexavalent chromium, Cr(VI):
- Highly toxic but valuable
- Priority pollutants defined by USEPA
- Electroplating, acid mining, refining, petroleum plants

Technologies for heavy metal treatment

- **Chemical precipitation**
  - *High equipment costs*
  - *Large consumption of reagents*
  - *Large volume of sludge*
  - *Ineffective recovery of treated metals*
  - *Potential hazard to environment*
- **Ion exchange**
  - *High capital and operating cost*
  - *Fouling*
  - *Pretreatment*
- **Activated carbon adsorption**
  - *Large intraparticle diffusion*
  - *High regeneration cost*
  - *Low regeneration efficiency*

Magnetic nanoparticle adsorption

Advantages	Implications for industrial applications
Comparatively large adsorption capacity	Superior removal
Very short adsorption time	Saved space, especially suitable for crowded cities
Easy to separate from treated water	Lower capital and operating costs
Simple to desorb	Easy technical adaptation and maintenance
No secondary pollution	No potential environmental concern

Maghemite nanoparticles for Cr(VI) removal

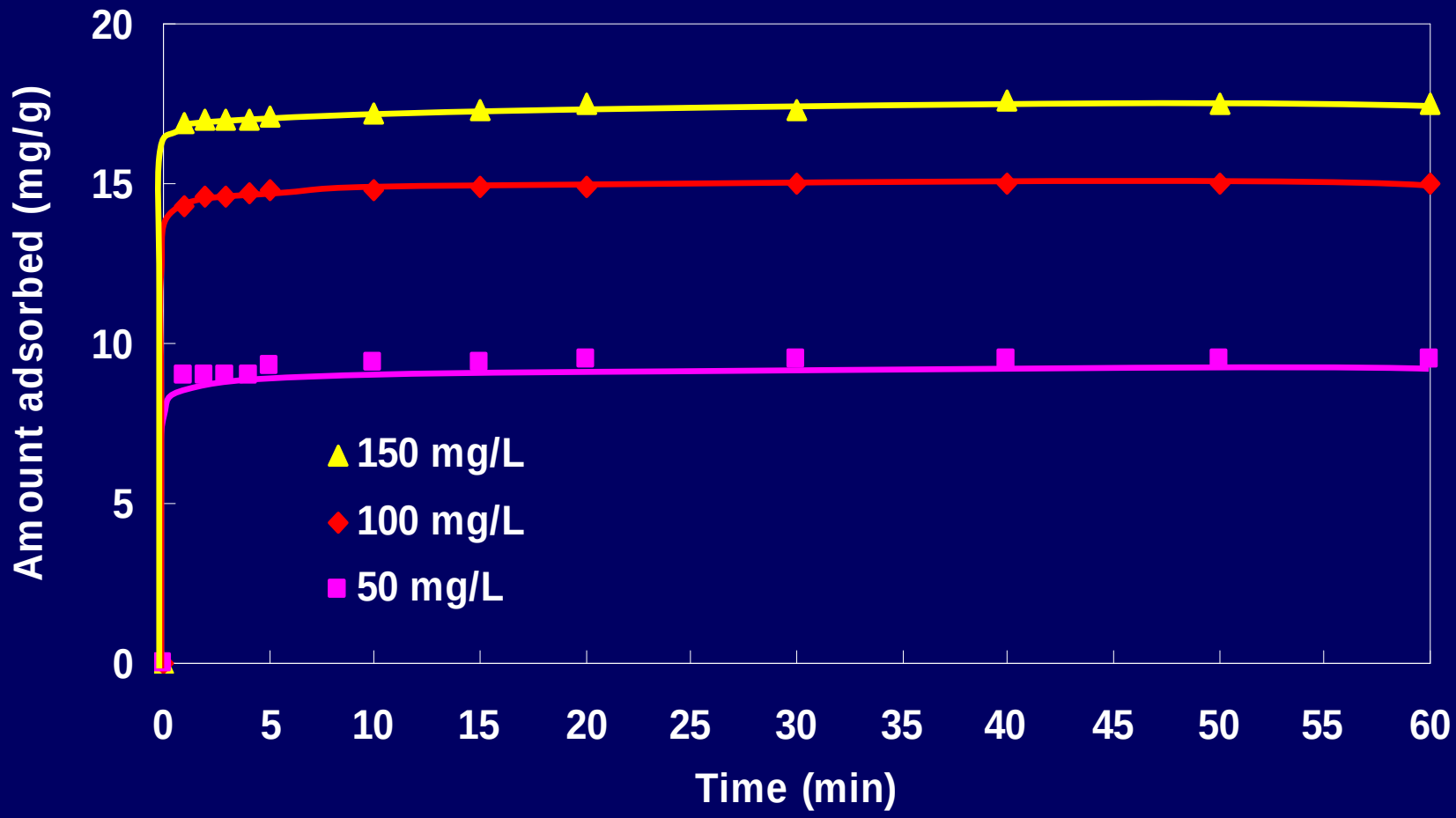

Cr(VI) adsorption equilibrium time = 10 min; 50 mg/L of Cr(VI) was reduced to be 0.05 mg/L, below discharge limit

How to enhance adsorption?

1. Metal-doping technique

- Increase in surface area or active sites
- Simple modification method
- Other parameters not impaired significantly, e.g., adsorption rate, magnetic properties
- Stable nanoparticles

2. Inorganic coating technique

Objectives

- Promotion of adsorption by metal-doping
- Inhibition of dissolution by metal-doping
- Mechanism studies by Raman spectroscopy

Materials and Methods

- **Adsorbent**

  Metal-doped γ-Fe_2O_3 nanoparticle (Me= Al, Mg, Cu, Zn, Ni)

- **Adsorbate**

  100 mg/L K_2CrO_4 + 0.1 M $NaNO_3$

- **Batch test**

  Experimental conditions: contact time: 60 min; pH: 2.5;
  shaking rate: 200 rpm; room temperature: 25^oC

- **Mechanism study**

  Sample for Raman: 5, 50, 100 mg/L Cr(VI) at pH 2.5, 6.5, 8.5

Analytical Methods

Parameters	Analytical methods
Cr	ICP
pH	pH Meter
Zeta potential	ZETA PLUS
Particle dimension	TEM
Particle structure	XRD
Elemental analysis	XRF
Complexation	Raman spectroscopy
Surface area	BET Analyzer
Magnetism	VSM

Raman spectroscopic studies

- Establish symmetry of surface species
- Distinguish inner-sphere from outer-sphere

  (David et al., 1978; Tejedor and Anderson, 1990)

- Raman spectroscopic data about PO_4^{3-}, CO_3^{2-}, SeO_4^{2-}, SO_4^{2-}, and AsO_4^{2-} adsorption onto Fe/Al oxides available

  (Schulthess and McCarthy, 1990; Su and Suarez, 1998; Wijnja and Cristian, 2000; Goldberg and Johnston, 2001)

- Little detailed information on Raman spectroscopic study of CrO_4^{2-} adsorption onto (modified) iron oxide

Modification of synthesizing methods

- **Precipitation method**

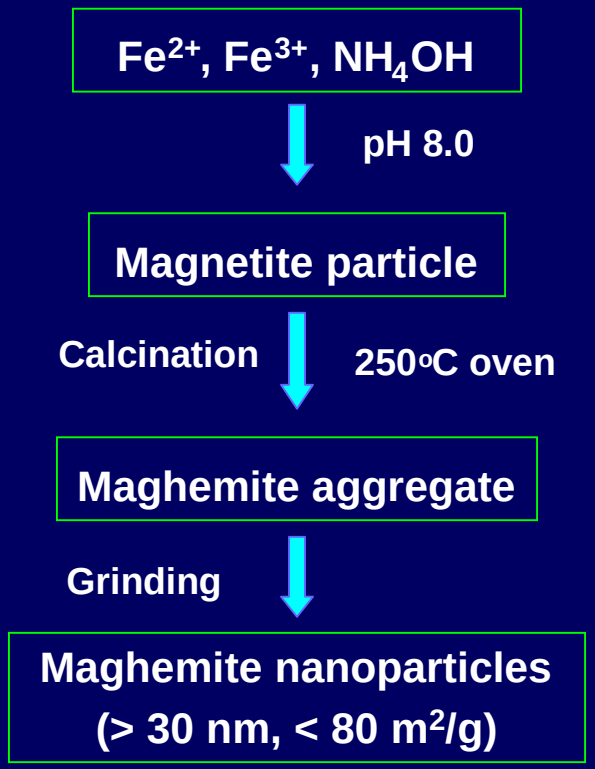

- **Sol-gel method**

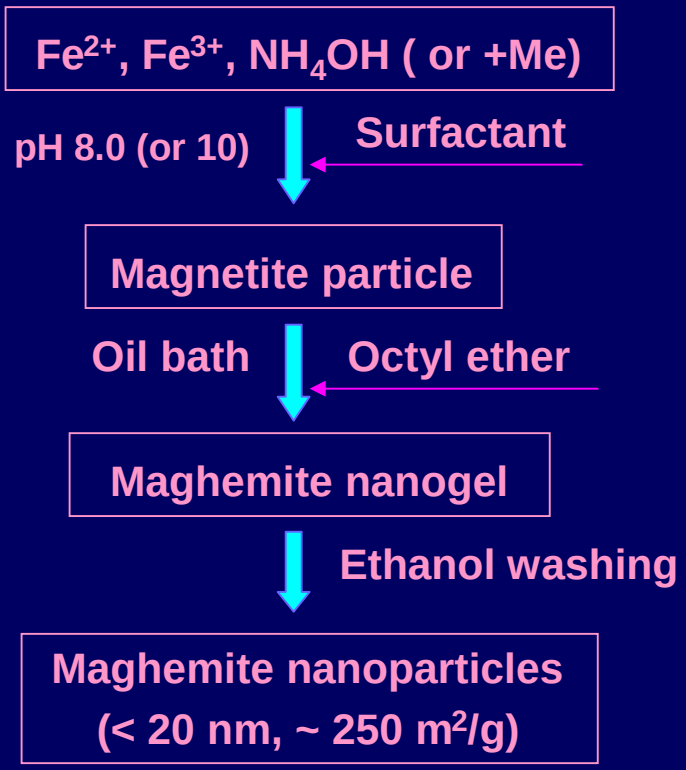

Nanoparticle Synthesis Method (sol-gel)

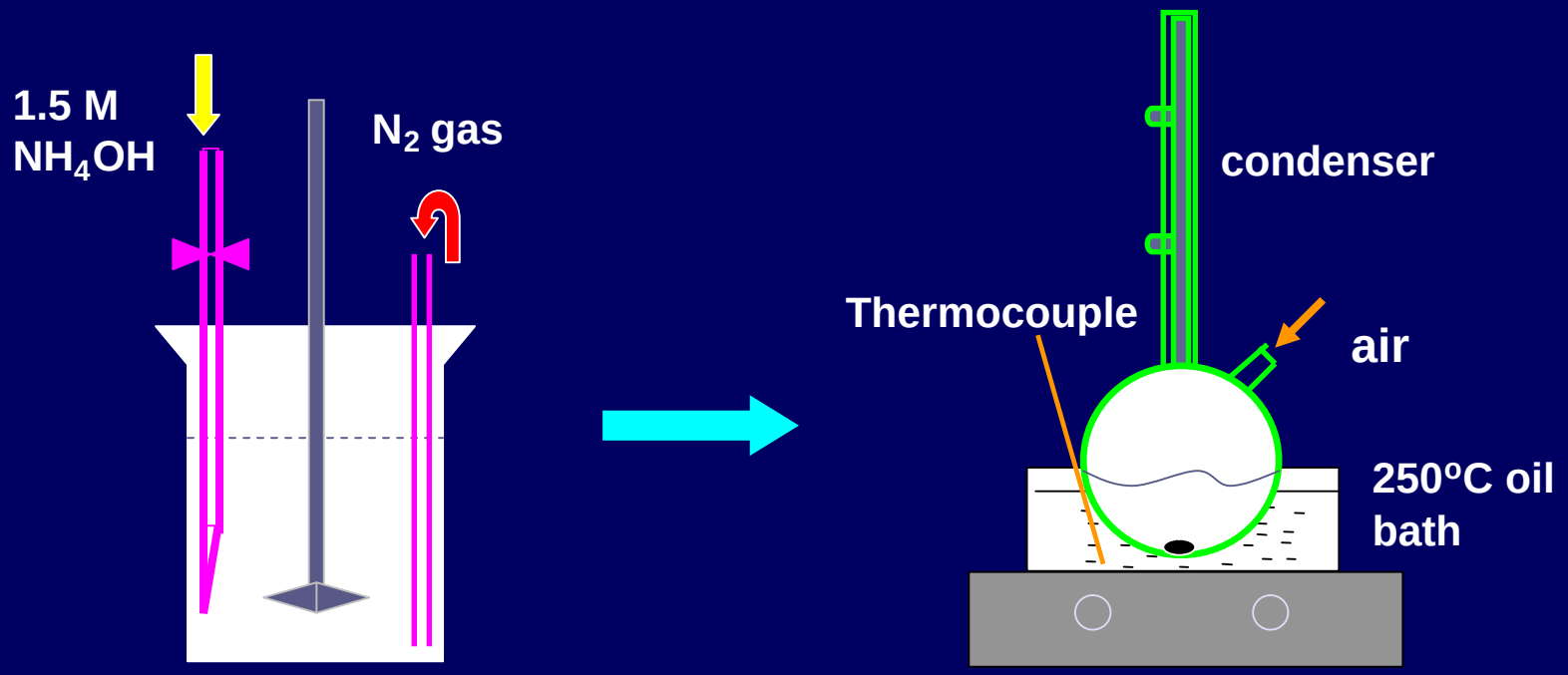

Al-doped magnetite (Fe_3O_4)

Al-doped maghemite (γ-Fe_2O_3)

TEM images of Al-doped γ-Fe_2O_3

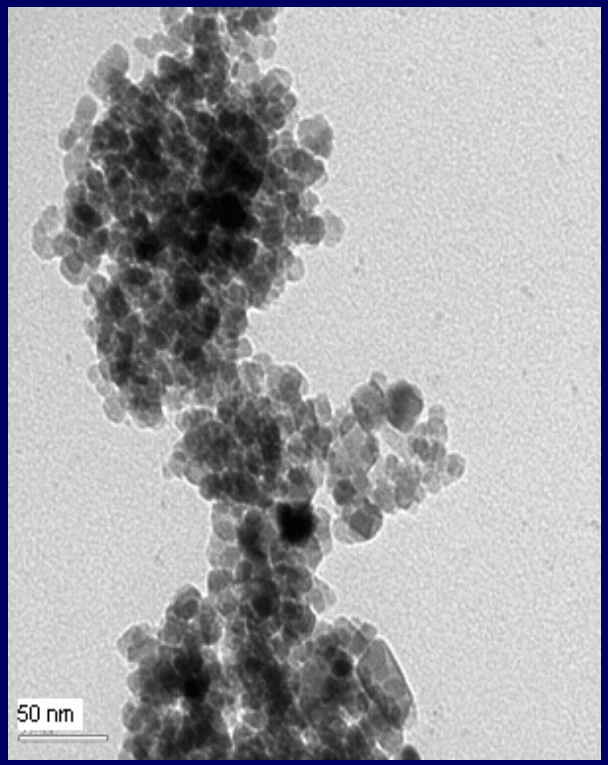

Undoped γ-Fe_2O_3

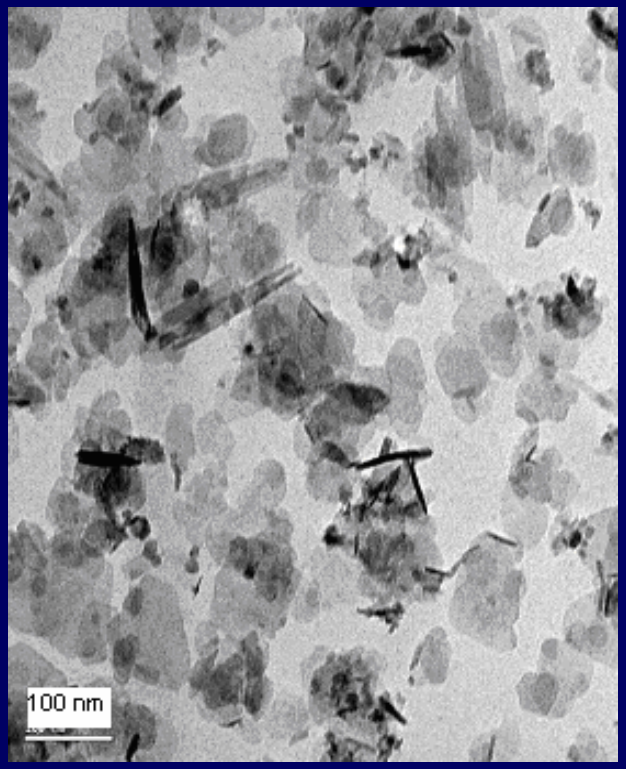

Al-doped γ-Fe_2O_3 with 7.5% of Al

Al-doped γ-Fe_2O_3 with 13.1% of Al

Doping of Al results in preferential crystal growth along [100] direction producing irregular shaped, platy particles, at expense of crystal thickness (Schulze, 1984)

XRD patterns of undoped & Al-doped γ-Fe_2O_3

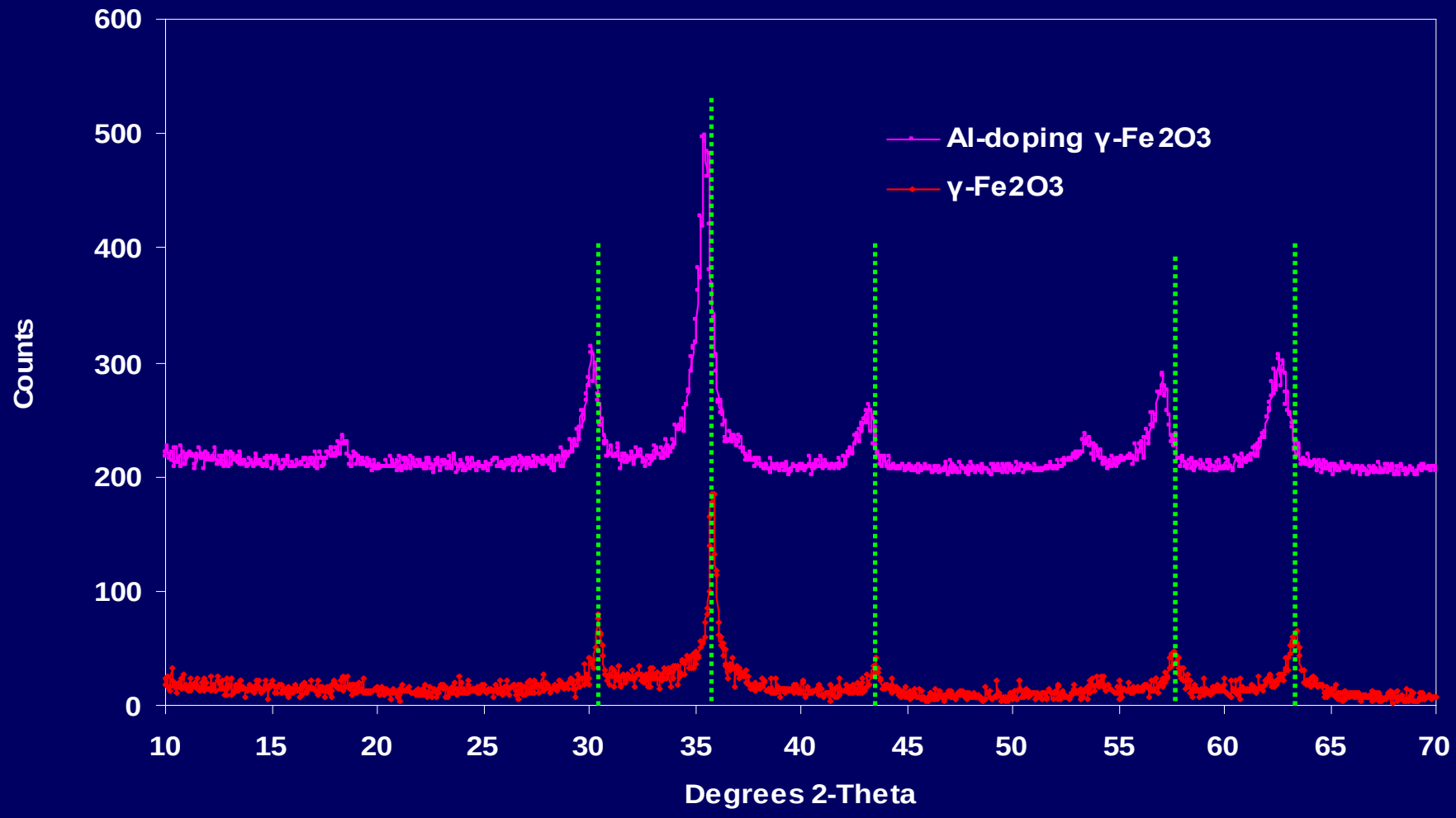

A definite proof of structural incorporation can be produced from a shift in position of XRD peaks, but doping would not change original structure

Hysteresis loops of Al-doped γ-Fe_2O_3

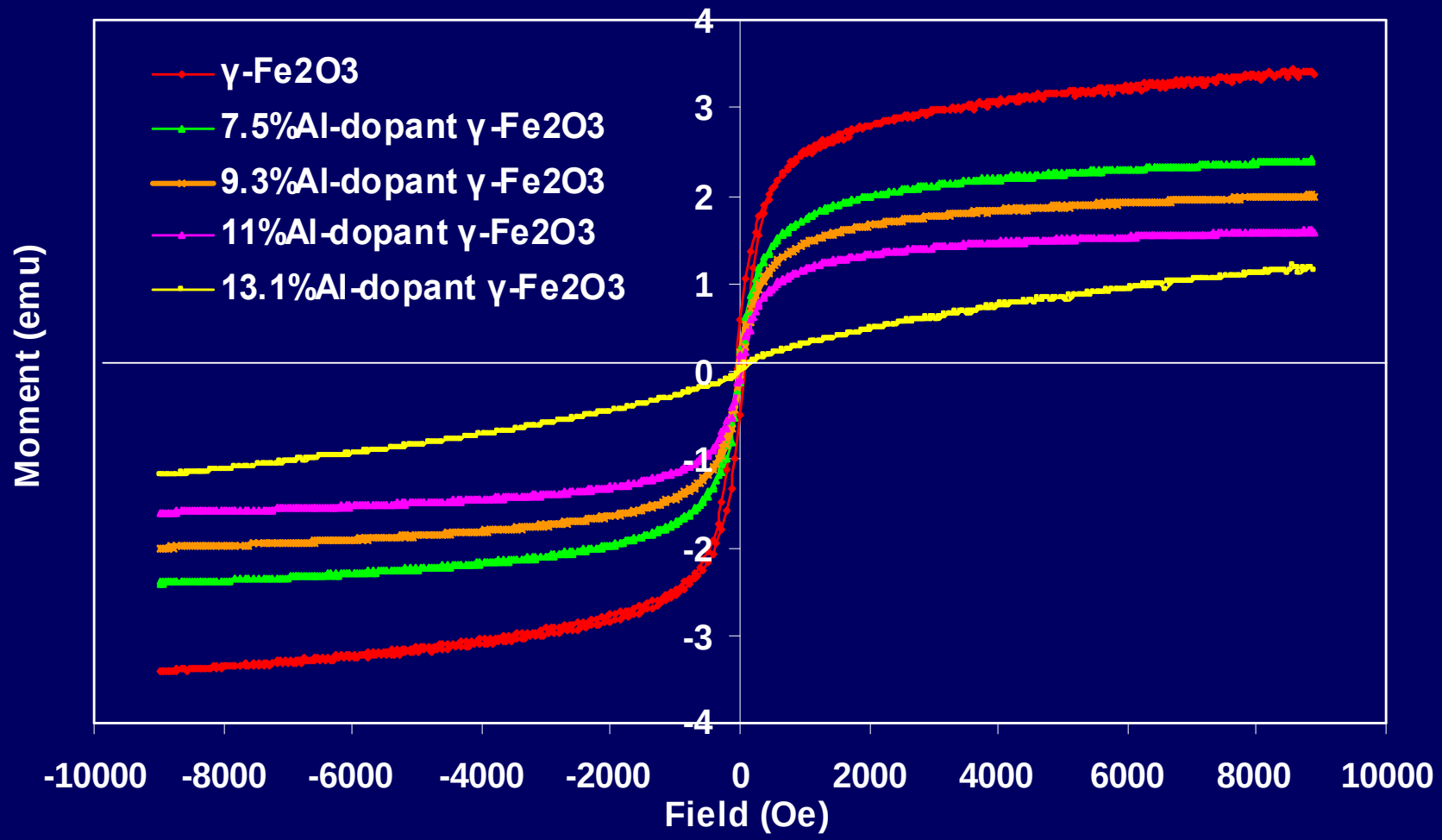

Magnetic properties decreased with increasing Al dosage

Effect of doped metal on Cr(VI) adsorption

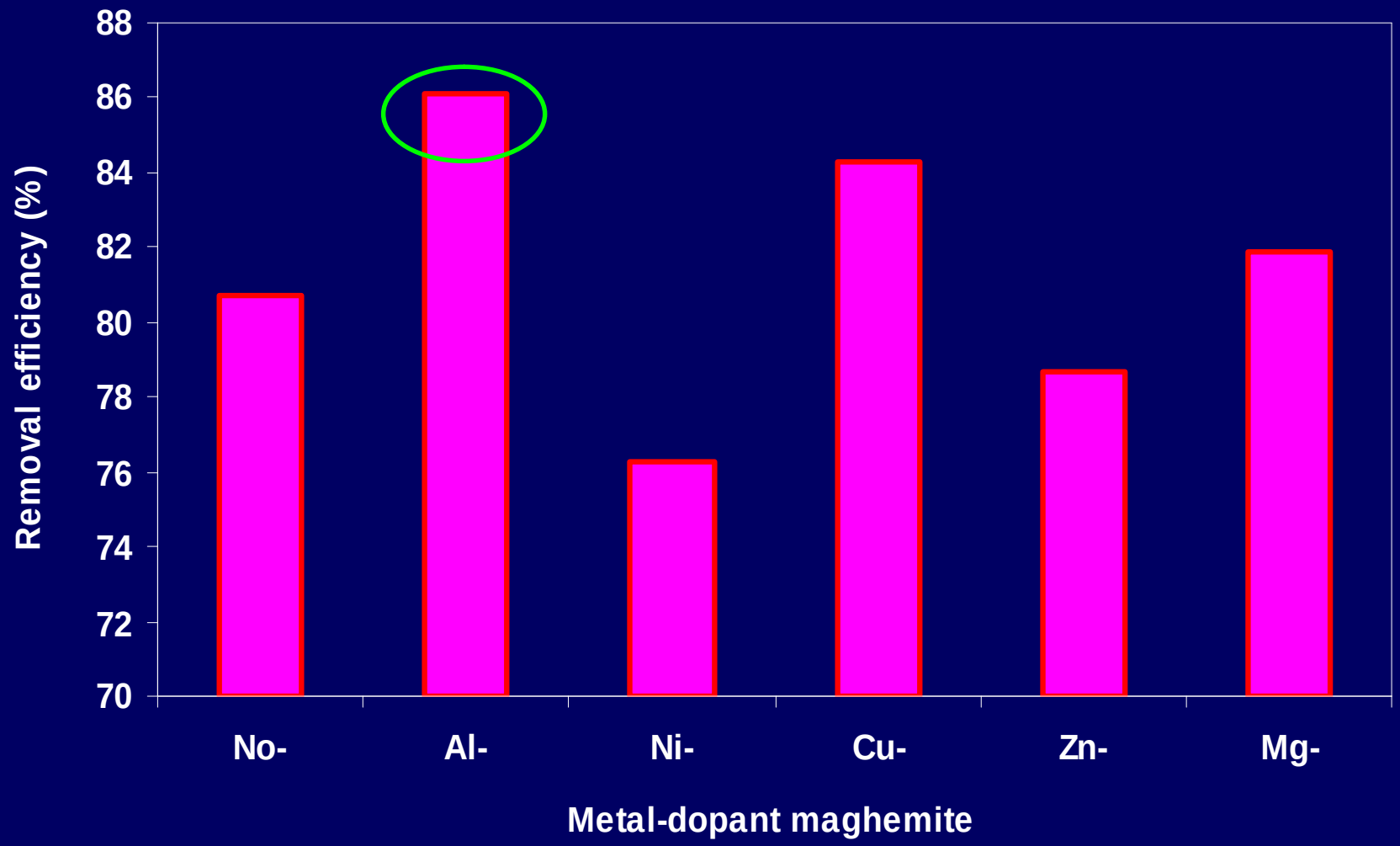

Al-, Cu- and Mg- doping enhanced adsorption capacity; while Cu- and Ni-doping decreased adsorption capacity of previous γ-Fe_2O_3

Adsorption and separation

Al/(Al+Fe)	Surface area	Adsorption efficiency	Equilibrium time	Magnetic properties	Separation Time
(%)	(m^2/g)	(%)	(min)	(emu)	(min)
0	162	79.8	10	3.48	0.1
7.5	182	84.3	25	2.26	0.5
9.3	191	86.7	30	1.78	1
11.0	198	87.5	60	1.14	5
13.1	210	88.9	90	/	10

Adsorption mechanism (Raman)

— Cr(VI) adsorption onto Al-doped γ-Fe_2O_3

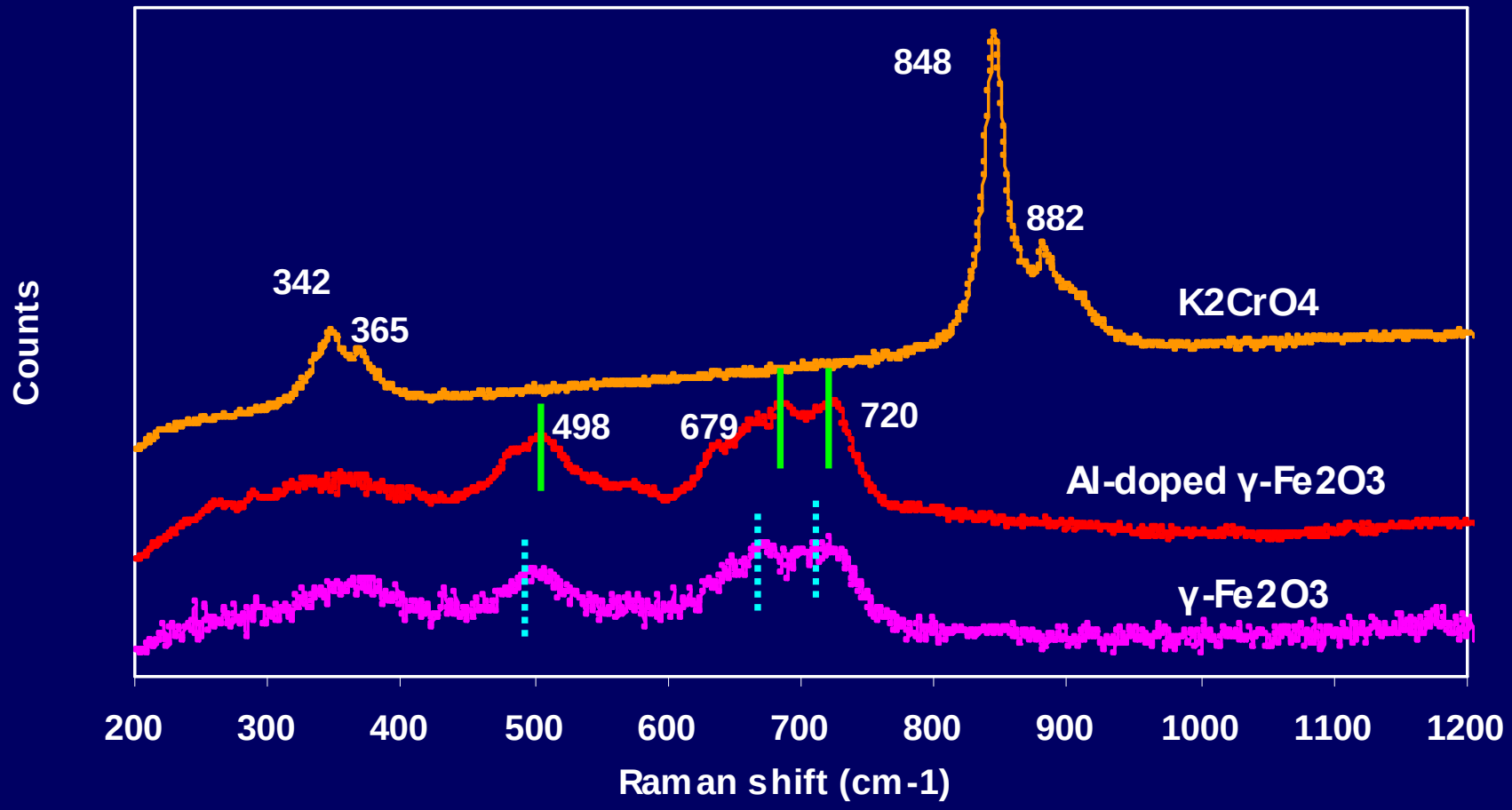

Vibrations for the free CrO_4^{2-} are all Raman active: the nondegenerate v_1 at 848 cm^{-1}, the doubly degenerate v_2 at 342 cm^{-1}, the triply degenerate v_3 at 882 cm^{-1}, and the triply degenerate v_4 at 365 cm^{-1}

Raman spectra

— Effect of pH

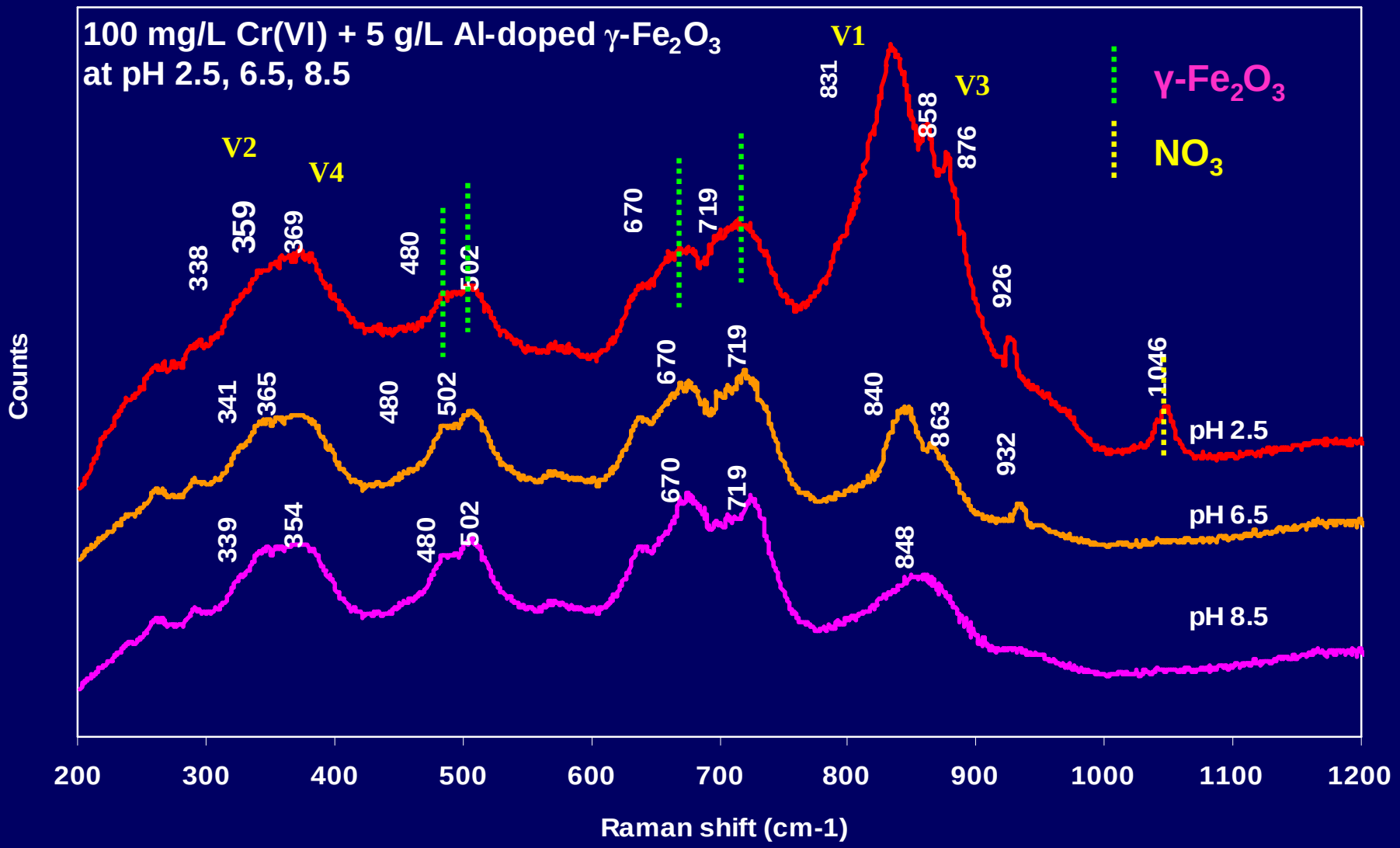

Raman spectra

— Effect of surface loading

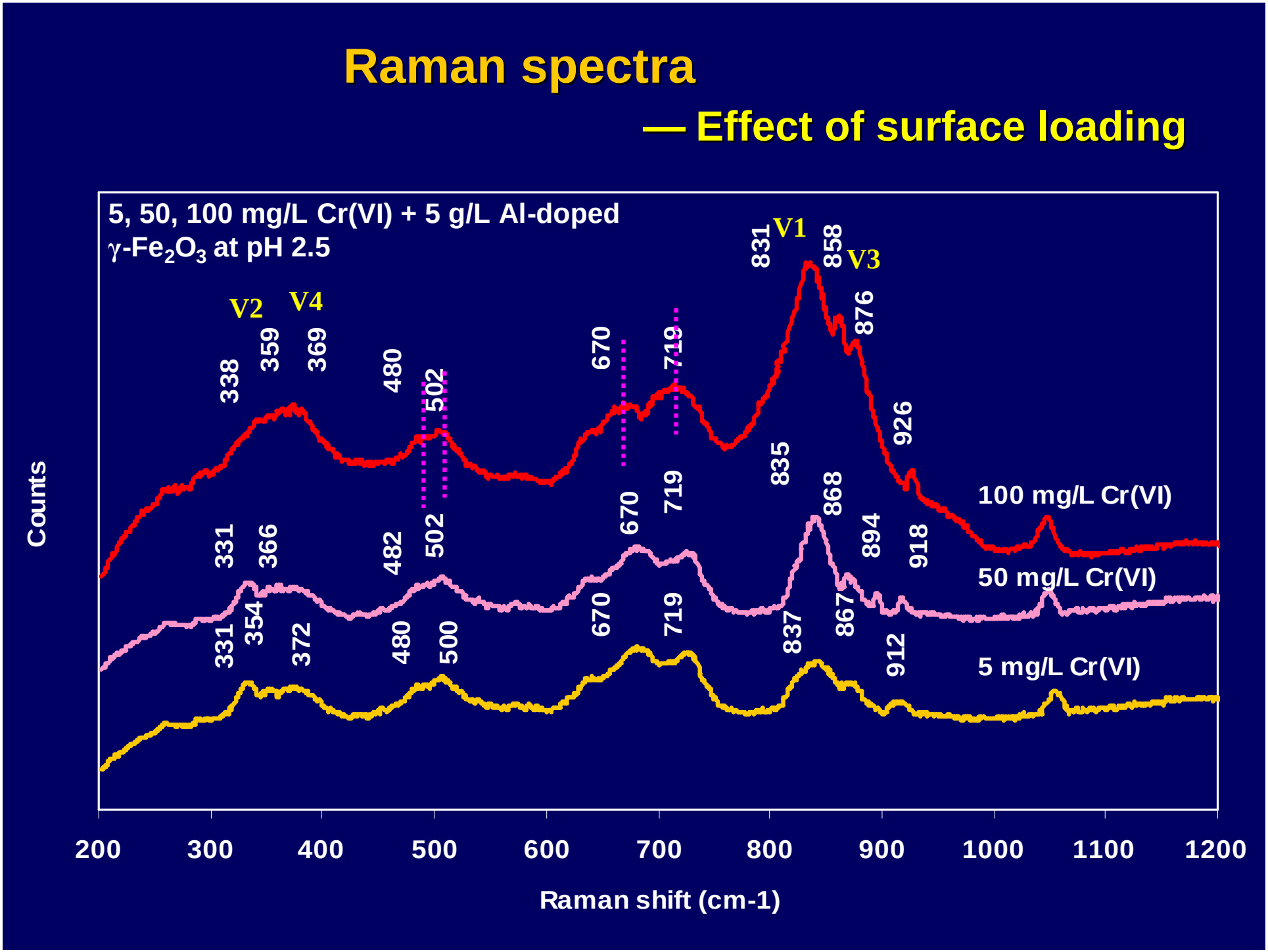

Vibrations between CrO_4^{2-} and Al-doped γ-Fe_2O_3

Species	Cr(VI) (mg/L)	pH	Frequency (cm^{-1})						
			ν_1	ν_2	ν_3			ν_4	
K_2CrO_4 (aq)			848	342	882			365	
Al-doped γ-Fe_2O_3	5	2.5	837	331	867	912		360	
Al-doped γ-Fe_2O_3	50	2.5	835	331	868	894		366	
Al-doped γ-Fe_2O_3	100	2.5	831	338	858	876	926	359	369
Al-doped γ-Fe_2O_3	100	6.5	840	341	863	932		365	
Al-doped γ-Fe_2O_3	100	8.5	848	339	/			354	

Inner-sphere complex between Cr(VI) and Al-doped γ-Fe_2O_3

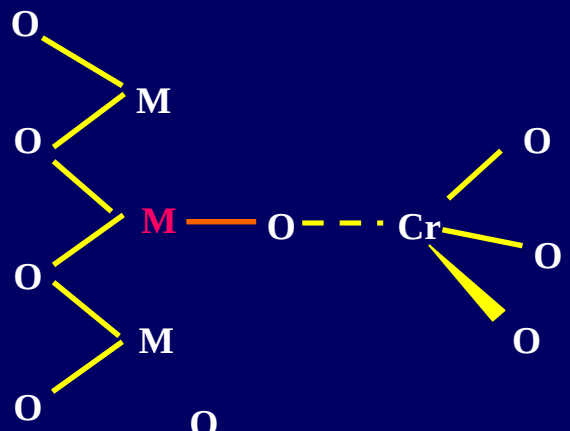

Monodentate

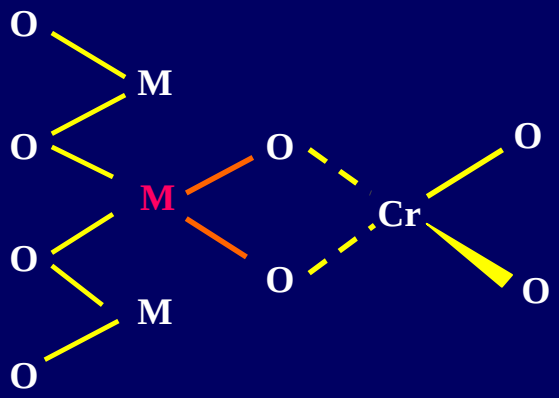

Bidentate mononuclear*

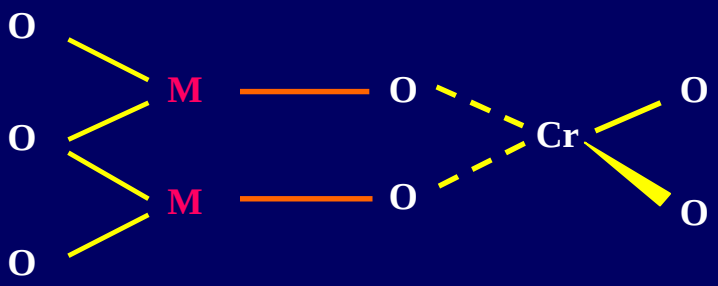

Bidentate binuclear*

Increasing pH

Increasing surface loading

(* Together with data from Hiemstra et al., 1989; McBride, 1994; Fendorf et al., 1997; Wijnja and Schuthess, 2000)

Adsorption isotherms

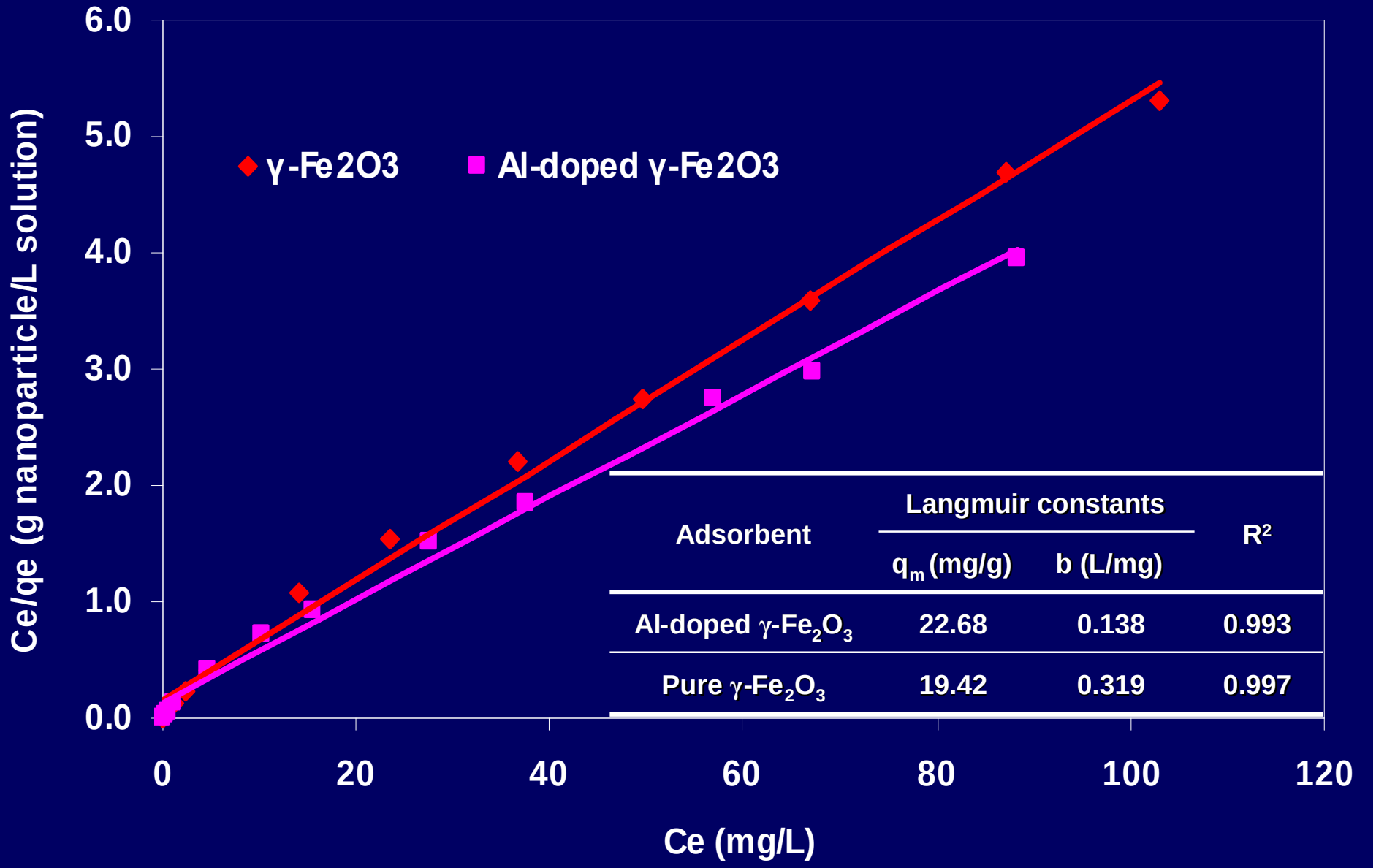

Adsorbent	Langmuir constants		R^2
	q_m (mg/g)	b (L/mg)	
Al-doped γ-Fe_2O_3	22.68	0.138	0.993
Pure γ-Fe_2O_3	19.42	0.319	0.997

Comparison of adsorbents

Type of adsorbents	q_m (mg/g)	Equilibrium time (h)	Optimum pH	References
Coconut tree sawdust	3.46	3	3.0	(Selvi et al., 2001)
Lignin	5.64	24	2.5	(Lalvani et al, 2000)
Distillery sludge	5.7	1.75	3.0	(Selvaraj et al., 2003)
Blast-furnace slag	7.5	6	1.0	(Srivastava et al., 1997)
Diatomite	11.55	2	3.0	(Dantas et al., 2001)
Aluminum oxide	11.7	8	4.0	(Gupta et al., 1999)
Anatase	14.56	24	2.5	(Weng et al, 1997)
Activated carbon	15.47	3	4.0	(Sandhya and Tonni, 2004)
Beech sawdust	16.13	1.33	1.0	(Acar and Malkoc, 2004)
Hazelnut shell	17.7	5	2.0	(Cimino et al.,2000)
Spent grain	18.94	8	2.0	(Low et al., 2001)
Al-doped γ-Fe_2O_3	*22.68*	*0.5*	*2.5*	*Present study*
Larch bark	31.25	48	3.0	(Aoyama and Tsuda, 2001)

Note: Cr(VI) Adsorption capacity and equilibrium time at room temperature of 22.5 ±2.5°C

Prevention of nanoparticle dissolution

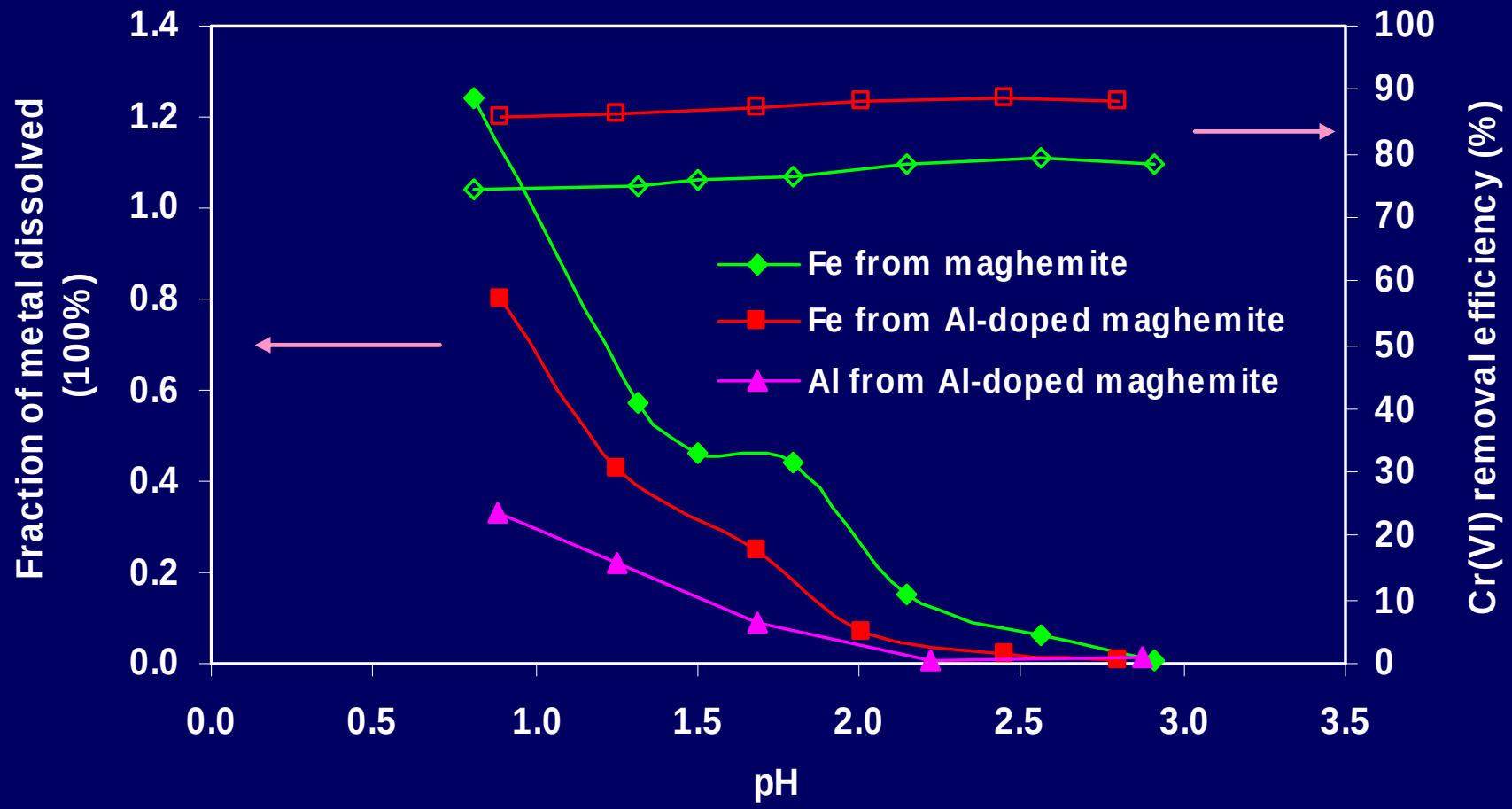

1) Al-O bond energy (513 kJ mol^{-1}) > Fe-O bond energy (390 kJ mol^{-1}),

2) More energy to remove simultaneously two center atoms due to effect of binuclear complexes (Cornell et al., 2003)

Conclusions

- Optimal Al dosage is ***9.3*** mol%
- Enhanced adsorption capacity from ***19.4*** mg/g to ***22.7*** mg/g by Al-doping
- ***Insignificant*** nanoparticle dissolution under experimental condition; Al-doping inhibited dissolution by ***30%***
- Complexation changed from outer-sphere into ***inner-sphere complexation*** by Al-doping


Thank you